

Depth Profiling of Ultrathin P(S-*b*-MMA) Diblock Copolymer Films by Selective Solvent Crazing

Svetlana Gourianova and Jürgen Fuhrmann*

Institute of Physical Chemistry, Technical University Clausthal, Arnold-Sommerfeld-Str. 4, D-38678 Clausthal-Zellerfeld, Germany

Received December 16, 2002

ABSTRACT: Selective solvent crazing is proposed as a novel method for depth profiling and obtaining three-dimensional information by AFM on the microphase morphology in ultrathin polystyrene/poly-(methyl methacrylate) (P(S-*b*-MMA)) diblock copolymer films on silicon substrate. To remove selectively one of the blocks, chain scission must be achieved within this block. Therefore, a proper chosen solvent has to cause selective swelling combined with crazing. Both effects depend on differences in the solubility parameters of the polymers relative to the solvent. As a complementary contrasting procedure for the P(S-*b*-MMA) diblock copolymer system, plasma etching, which preferentially degrades PMMA, is used. For the same system a solvent crazing of the PS block is proposed with cyclohexane as a crazing agent. The novel procedure gets of special importance if the solvent-dependent morphology of spin-cast ultrathin diblock copolymer film can be inverted, e.g., if PMMA islands in a PS matrix spin-cast from toluene solution are inverted to PS islands in a PMMA matrix spin-cast from methyl ethyl ketone (MEK) solution. Again, the phase inverting solvent has been selected by help of the solubility parameters.

Introduction

Environmental crazing of polymeric materials in the presence of an organic liquid or vapor is a well-known phenomenon, which may manifest itself even without the presence of external mechanical stress.^{1–5} It results from local heterogeneity of composition and/or local anisotropy of molecular orientation, which can lead to high stress or strain concentration caused by solvent diffusion, i.e., when a time varying solvent concentration profile superposes a heterogeneity profile. Solvent crazing may be regarded as an inherent material weakness of glassy polymers.¹ Some of the previous work has focused on the nature of the polymer–solvent interaction, specifically on the solubility parameters of the solvent and polymer, and it was shown that a crazing agent may be selected for a glassy homopolymer by inspecting the solubility parameters of possible solvents.^{3,6}

In the case of glassy block copolymers we propose to select a solvent that acts as both crazing agent and selective dissolution agent for one of the block copolymer components. If both conditions are handled by using the solubility parameters in a proper way, then this block can be removed by selective solvent crazing. This allows to obtain the three-dimensional information on microphase morphology in thin block copolymer films and depth profiling by atomic force microscopy (AFM). An important aspect of these investigations is the possible chain scission as a prerequisite for preferential dissolution of one of the block phases. Diblock junction is mainly located within the interphase between neighboring segregated block phases.⁷ The interphase acts as a barrier of the swelling as well as for the chain scission and for selective dissolution.

A method for analyzing a given segregated block copolymer system by means of solvent treatment can

be established in a two-step selection procedure: first, a solvent for selective dissolution of one block copolymer component should be chosen; second, one should make sure that this solvent acts as an solvent crazing agent.

Ultrathin spin-cast P(S-*b*-MMA) diblock copolymer films on silicon substrate are taken as examples for the proposed microdomain contrasting procedure. To remove the PMMA microphase air plasma etching has already been used successfully.^{8–11} We have used a new solvent etching procedure for the removal of the PS microphase. The three-dimensional information obtained by selective solvent crazing has been compared with the information obtained by selective air plasma etching.

Selection of Solvents. The solubility parameter was used as an adjusting parameter for the choice of solvents for the spin-casting and for the subsequent contrasting procedure; i.e., the selection of solvents addresses two different phenomena: (i) one solvent addresses the microphase formation by spin-casting of the ultrathin block copolymer film on silicon substrate, and (ii) the other solvent addresses the contrasting of the microphase domain structure of that film.

A diblock copolymer film prepared from solution by spin-casting may be in a nonequilibrium microphase structure with each of the microphases in a glassy state. Therefore, the glassy microphase-separated structure depends on the solvent used in the spin-casting processes. The intended nonequilibrium morphology features may be realized by means of Hansen's solubility parameters of the solvent and the copolymer, which quantify the polymer–solvent interaction.¹²

In the description of polymer–liquid interactions proposed by Hansen,¹³ each polymer (*j*) and solvent (*i*) is characterized by a set of three parameters (Hansen parameters) designated by subscripts *d* (dispersion), *p* (polar), and *h* (hydrogen bonding), according to the type of the interactions they reflect. The region of solubility is characterized by the difference between

* To whom the correspondence should be addressed: Tel +49 5323 72 2204, +49 5323 72 2788; Fax +49 5323 72 2863; e-mail fuhrmann@pc.tu-clausthal.de.

Table 1. Solubility Parameter δ and the Dispersion δ_d , Polar δ_p , and Hydrogen-Bonding δ_h Components of Polymers (PS and PMMA) and Solvents (Cyclohexane and MEK)^{13,14}

	δ [MPa ^{1/2}]	δ_d [MPa ^{1/2}]	δ_p [MPa ^{1/2}]	δ_h [MPa ^{1/2}]
PS	22.47	21.28	5.75	4.3
PMMA	22.69	18.64	10.52	7.51
cyclohexane	16.8	16.8	0	0.2
MEK	19.0	16.0	9.0	5.1

solvent and solute solubility parameter:^{13–15}

$$R_{ij} = (4(\delta_{id} - \delta_{jd})^2 + (\delta_{ip} - \delta_{jp})^2 + (\delta_{ih} - \delta_{jh})^2)^{1/2}$$

The smaller this difference, the better is the polymer solubility in the solvent. The “total” cohesion parameter, δ_t , of either polymer or liquid, given by $\delta_t = (\delta_d^2 + \delta_p^2 + \delta_h^2)^{1/2}$, corresponds to the Hildebrand parameter.

The nature of the solvent influences the degree of the swelling of the polymer chains in each domain and hence an effective volume fraction of each domain.¹⁶ The microphase-separated structure, which exists already in the solution, determines the nonequilibrium structure in the film obtained after complete solvent evaporation. This is the result of the high evaporation speed of the solvent compared to the speed of structural relaxation in the microphase-separated system.¹⁷ For example, toluene is a better solvent for PS than for PMMA, and the P(S-*b*-MMA) diblock copolymer highly diluted in toluene has a partially segregated PMMA core and a PS shell.¹⁸ Thus, from toluene solutions one gets spin-cast block copolymer films with PMMA islands embedded in a continuous PS-block microphase.¹¹ In contrary to this morphology, we aimed at PS islands in a PMMA block microphase. Therefore, we have chosen methyl ethyl ketone (MEK) as a solvent, which has solubility parameters good for PMMA and weak for PS (Table 1). The difference between MEK and PS solubility parameters ($R_{\text{MEK/PS}}$) is 11.1 MPa^{1/2}, and the difference between MEK and PMMA solubility parameters ($R_{\text{MEK/PMMA}}$) is 6.0 MPa^{1/2}. MEK is a better solvent for PMMA than for PS; thus, it should lead to PS island morphology in ultrathin spin-cast P(S-*b*-MMA) films.

According to the contrasting phenomenon, we choose cyclohexane. Cyclohexane should act as crazing agent on PS islands embedded in glassy PMMA matrix in a spin-cast ultrathin film on silicon substrate and should be able to show selective dissolution of PS block copolymer component. The solubility parameters of this solvent are listed in Table 1. The difference between cyclohexane and PS solubility parameters ($R_{\text{Ch/PS}}$) is 11.4 MPa^{1/2}, and the difference between cyclohexane and PMMA solubility parameters ($R_{\text{Ch/PMMA}}$) is 13.3 MPa^{1/2}. Cyclohexane is a Θ solvent at 34.5 °C for PS and a nonsolvent for PMMA.¹⁴ The selectivity of cyclohexane toward PS in a PS/PMMA system has been shown by Krausch et al.,¹⁹ who used this solvent for selective dissolution of the linear PS component in a PS/PMMA blend. Also, Russell et al.²⁰ investigated the penetration of cyclohexane vapor into ordered multilayers of symmetric PS/PMMA diblock copolymers by neutron reflectivity and observed only a swelling of the PS layer at the free surface. The underlying multilayered structure was unperturbed by the solvent vapor. This result indicates that the first PMMA layer near the surface acts as an effective diffusion barrier, preventing penetration of the cyclohexane.

Vincent and Raha³ examined the stress crazing of some homopolymers in the presence of liquid environments. It was shown that hydrogen bonding is an important factor, which must be considered for the explanation of crazing behavior of a polymer. To generalize the results of Vincent and Raha, Van Krevelen et al.¹ plotted their data in a $\delta_{\text{VS}} - \delta_{\text{VP}}$ vs $\delta_{\text{HS}} - \delta_{\text{HP}}$ diagram with $\delta_v = ((\delta_d)^2 + (\delta_p)^2)^{1/2}$. The subscripts S and P denote solvent and polymer. There is a small zone near the center ($\delta_{\text{VS}} \approx \delta_{\text{VP}}$; $\delta_{\text{HS}} \approx \delta_{\text{HP}}$), where all solvents dissolve the polymer. At a large distance from the center, crazing is generally found. In the intermediate zone, the main phenomenon is solvent cracking, although dissolution, swelling, or crazing is observed with some solvents. This diagram permits the prediction of solvent behavior. Cyclohexane is in the intermediate zone, nearer to the boundary with crazing region for PS, and in the crazing region for PMMA. Vincent and Raha³ and Kambour et al.² investigated cyclohexane as crazing agent for PMMA and PS, respectively, and determined the critical strains ϵ_c for solvent crazing of PS (0.13%) and of PMMA (1.10%). The critical strain of solvent crazing ϵ_c was assumed to be the minimal value of strain, at which the appearance of the first craze was observed. It may be estimated by bending polymer sheet in an active liquid.³ According to crazing agents classification of Vincent and Raha, cyclohexane is a high-strain crazing agent for PMMA and low-strain crazing agent for PS, i.e., a stronger crazing agent for PS.

Experimental Section

Diblock Copolymer. The symmetric diblock copolymer P(S-*b*-MMA) used in this work, courtesy of R. Stadler, is described elsewhere.²¹ The molecular weights of the styrene and the methyl methacrylate blocks are 128 and 147 kg/mol, respectively; $M_w/M_n = 1.11$, and it is denoted as SM120. The weight fraction of the polystyrene block measured by ¹H NMR amounts to $w_{\text{PS}} = 0.4$.

Sample Preparation. The copolymer films were prepared by spin-casting a 5 μ L droplet of a MEK solution with concentration 2.5 g/L at room temperature and ambient conditions onto the silicon substrate, already rotating at 4500 rpm, as described elsewhere.¹¹ The substrate (about 5 mm \times 5 mm) was cut from a highly polished silicon wafer and cleaned with a precision wipe and with air plasma. The spin-cast films were dried in a vacuum for 4 h at 50 °C.

Plasma Treatment. The plasma cleaning of the substrate and the sample etching were performed in HAARICK (PDC-32G) plasma cleaner. For substrate cleaning a power of 60 W was used for about 20 min. For selective etching the PMMA microphases, a power of 40 W was used for about 20 s. The air plasma was regulated by controlling the air pressure to obtain the brightest plasma luminosity. After each etching period the samples were kept in a vacuum for an additional 15 min.

Atomic Force Microscopy. The ultrathin diblock copolymer films were measured by atomic force microscopy, using Tapping Mode while simultaneously recording the topography and the phase shift of the cantilever oscillation to obtain a material contrast. The AFM measurements presented in this paper were all made by a Multi Mode scanning probe microscope, Nanoscope III, Digital Instruments. We used Tapping Mode silicon tips with a cantilever length of 125 μ m (Nanosensors). All pictures were taken with light tapping²² ($A_0 \approx 70$ nm; $r_{\text{sp}} > 0.8$) from an area located 1 mm around the rotational axis given in the spin-casting process.

To obtain information about the absolute film thickness relative to the substrate, the films were scratched. The AFM tip was adjusted to a surface reference point, e.g., an intersection of two scratches, using an optical microscope and the samples were imaged by the AFM. Then the samples were

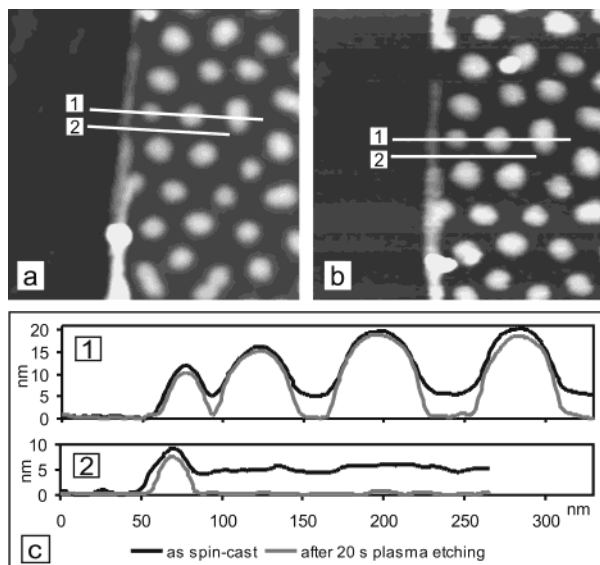


Figure 1. AFM topography images of a ultrathin P(S-*b*-MMA) diblock copolymer film on silicon substrate, spin-cast (4500 rpm) from MEK solution (2.5 g/L) (a) as spin-cast, (b) after 20 s of selective etching in air plasma, and (c 1, 2) the superimposed cross sections of topographic images before and after plasma etching taken at the positions indicated by white lines (1 and 2) in (a) and (b). AFM image size: 544 nm \times 544 nm. Data scale: height (a, b) 20 nm.

treated by air plasma or solvent. After that the samples were again adjusted under the AFM tip as described above, and an AFM picture of the identical surface area was taken. A comparison of the cross sections of the two topography images yields the information on the polymer composition profile inside the sample.

Results and Discussion

The topography of an ultrathin P(S-*b*-MMA) film on silicon substrate spin-cast from MEK solution is shown in Figure 1a. The dark area on the left-hand side of the image displays the bare silicon substrate after removal of the polymer film by a scratch. The topography image exhibits round elevated islands in a continuous matrix. The elevated domains have an average diameter of about 55 nm and a lateral periodicity of about 77–80 nm that is comparable to the domain period L of 72–79 nm as predicted for the bulk diblock SM 120.²³ To obtain information on the morphology inside the diblock copolymer film, two methods were used: selective plasma etching the PMMA microphases and selective solvent crazing the PS microphases.

Selective Plasma Etching. PMMA is known to be etched in air plasma faster than PS.^{9–11} The as spin-cast sample shown in Figure 1a was subsequently etched for 20 s in air plasma, and an AFM picture of the identical area was taken (Figure 1b). A cross section (Figure 1c) of the film before (Figure 1a) and after 20 s of selective plasma etching (Figure 1b) reveals that the about 5 nm thick continuous phase was removed down to a substrate, while the elevated islands remain almost unaffected during this etching time. This result allows us to assign the elevated islands to the PS-rich microphases.

In the case of ultrathin films spin-cast from toluene solution it has been shown that the PMMA microphases are higher than the PS continuous phase.¹¹ The films from MEK solution have an inverse structure. Depending on the relative solubility of the two block compo-

nents in their common solvent, PMMA phase shows a stronger swelling response in MEK than PS phase. This thermodynamic property leads to the formation of the PS microphases in the surrounding PMMA matrix during the spin-coating process. During evaporation of MEK the PS is more quickly depleted of the solvent.¹⁹ Subsequent evaporation of the residual MEK from PMMA leads to a collapse of the better soluble PMMA phase, and this leads to elevated PS islands.

Figure 2a,b shows the topography and the corresponding phase contrast of a sample spin-cast identically to the one in Figure 1a. The phase contrast (Figure 2b) reveals that the composition of the islands differs from that of the surrounding matrix, confirming the result obtained by etching procedure. The islands are dark, and the continuous phase is bright in the phase shift image. That means that under the given conditions of the AFM measurement the PMMA microphases appear brighter than PS microphases in the phase shift image.

Because of the AFM tip geometry, we cannot answer the question of whether the domains remaining after plasma etching have a convex or concave structure near the surface of the silicon substrate. In the case of diblock copolymer films characterized by PS domains in continuous PMMA matrix the question cannot be answered by the selective plasma etching without additional experiments, whether the PS domains are situated directly on the silicon substrate or a thin PMMA layer covers the substrate. An alternative etching method sensitive to PS will help to answer this question.

Selective Solvent Crazing. To obtain the complementary information on microphase morphology of the ultrathin P(S-*b*-MMA) diblock copolymer film spin-cast from MEK solution, the as-spin-cast sample (Figure 2a,b) was treated with cyclohexane (see “Selection of Solvents”) for morphological analysis.

Before the immersion in cyclohexane, the sample was exposed to cyclohexane atmosphere at room temperature. During the vapor exposure all PS blocks remain on the film surface independently of whether chain scissions occur. After removal from the cyclohexane vapor the sample was dried in a vacuum, and the identical area as before treatment was measured by AFM (Figure 2c,d). The diblock copolymer film morphology is strongly modified by the vapor treatment: the initial elevated domains are eliminated and hollows with elevated rims at the edge are left behind. From a comparison of the cross sections (Figure 2g) of the film before (Figure 2a) and after the cyclohexane vapor treatment (Figure 2c), it can be seen that PS material spreads laterally on the film surface, forming a layer decorating the PMMA phase. In the phase shift image the continuous phase and the hollows in the middle of the rims are dark (PS), and the rims are somewhat brighter. From Figure 2g it is clear that the diameter of the rims is comparable to the diameter of the initial domains. The morphology after cyclohexane vapor treatment is a result of the confined relaxation of the PS chains caused by the nonequilibrium of the as-spin-cast film.

The fact that the PS material remains on the film surface during the vapor exposure can be used for the comparison of PS amount on the surface before and after additional sample immersion in cyclohexane for the selective dissolution of the PS block. The sample was immersed in cyclohexane at 25 °C for 168 h. (Additional investigations showed that the visible changes of the

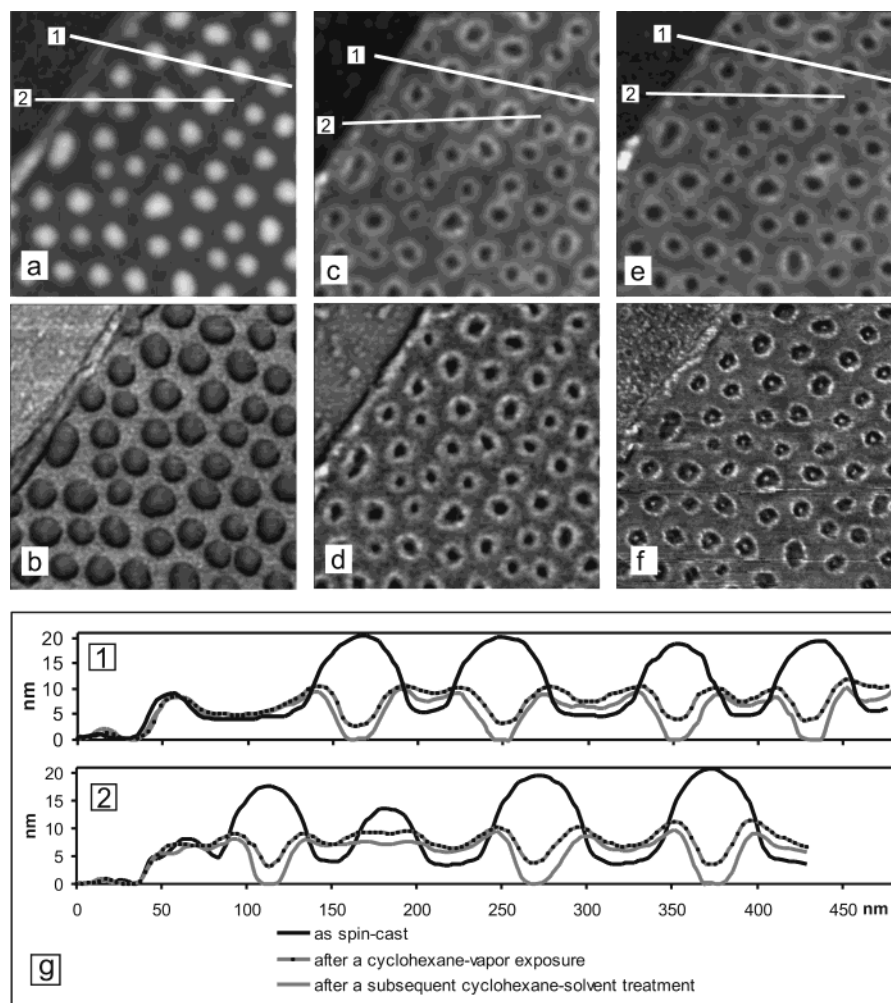


Figure 2. AFM topography images (a, c, e) and phase contrast images (b, d, f) of an ultrathin P(S-*b*-MMA) diblock copolymer film on silicon substrate, spin-cast (4500 rpm) from MEK solution (2.5 g/L) (a, b) as spin-cast, (c, d) after an exposure to cyclohexane vapor for 3 h at 25 °C (dried 2 h at 50 °C in a vacuum), and (e, f) after an subsequent immersion in cyclohexane solvent for 168 h at 25 °C (dried 2 h at 50 °C in a vacuum). The white lines (1 and 2) in topographic images (a, c, e) indicate the positions, where the cross sections (g 1, 2) were taken. AFM image size: 615 nm \times 615 nm. Data scale: height (a) 30 nm, (c, e) 15 nm; phase shift (b) 6°, (d) 15°, (f) 10°.

initial morphology of the spin-cast films occur already after an immersion time of some minutes, but the desired result of dissolution can be achieved only after a longer immersion time.) After immersion the sample was dried in a vacuum, and the same area was scanned again by AFM (Figure 2e,f). Because of the unaffected PMMA microphase arrangement, the topographic image looks similar to the image obtained after treatment in cyclohexane vapor. On the other hand, the surface profiles show large differences as can be seen from the comparison of the cross sections of the film after cyclohexane vapor treatment (Figure 2c) and after subsequent immersion in cyclohexane (Figure 2e) shown in Figure 2g. After immersion the film thickness becomes smaller than the film thickness after vapor treatment, and this is at all places of the film. The polymer material can be reduced only by chain scission, i.e., by the dissolution of the cleaved chains of the PS blocks in cyclohexane. We expect that all the cleaved PS chains are dissolved in cyclohexane, whereas the remaining PS blocks must be still bonded to the PMMA blocks.

Figure 2g shows that the initially elevated domains have lost their material after immersion in cyclohexane down to the substrate, generating uncovered parts of the substrate surface. In the phase contrast (Figure 2f)

the uncovered substrate is detectable as a bright points in the center of the deepest hollows. Presumed that the PMMA phase keeps the initial morphological structure during cyclohexane treatment, we can conclude that the initial elevated domains extend down to the substrate. This result is unexpected; because of surface free energy reasons, PMMA should cover the silicon substrate completely. Using the plasma etching technique, one get no chance to elucidate the PS-covered morphology of PMMA phase. But with the help of the cyclohexane immersion technique one can remove the covering PS and investigate the PMMA phase morphology.

Annealing. To confirm the assumption of solvent crazing of the PS block and to prove the selective dissolution of the resulting linear PS, two samples, an untreated one and a sample immersed in cyclohexane at 25 °C for 168 h, were annealed at 150 °C for 21 h (Figure 3). The initial symmetric diblock copolymer gets asymmetric due to chain scission, and this influences the equilibrium morphology of ultrathin block copolymer film. From Figure 3 it is clear that the morphological structures of the films achieved during the annealing show significant differences.

It is known that the morphology of ultrathin symmetrical P(S-*b*-MMA) diblock copolymer films with the

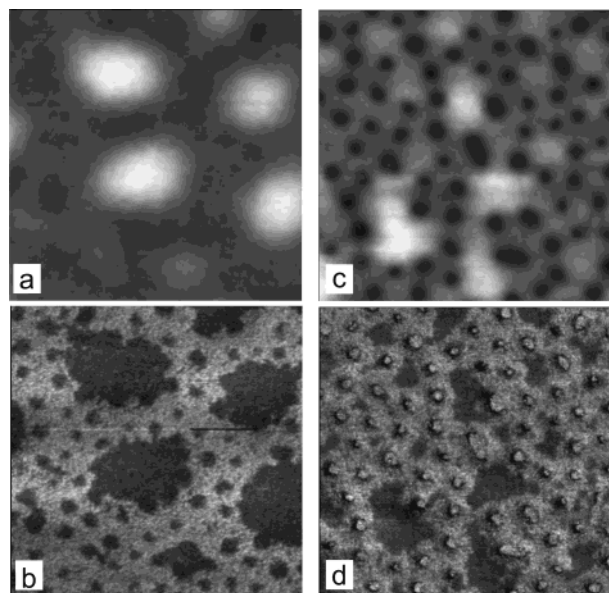


Figure 3. Topographies (a, c) and phase contrast images (b, d) of the ultrathin P(S-*b*-MMA) diblock copolymer films on silicon substrate, spin-cast (4500 rpm) from MEK solution (2.5 g/L) (a, b) after annealing for 21 h at 150 °C and (c, d) after an immersion in cyclohexane for 168 h at 25 °C (dried 2 h at 50 °C in a vacuum) and subsequent annealing for 21 h at 150 °C. Image size: 1 $\mu\text{m} \times 1 \mu\text{m}$. Data scale: height 20 nm; phase shift 10°.

film thickness smaller than $L/2$, where L is a domain period in the bulk, consists after annealing of PS-rich islands on a continuous PMMA-rich layer located at the interface to the silicon substrate.²⁴ Because of the limited annealing time, the films in Figure 3 did not yet achieve the equilibrium state, but a greater part of the PS blocks accumulated already on the film surface forming islands. So it became possible to compare quantitatively the volume of the PS islands in the untreated film (Figure 3a,b) and film after immersion

Table 2.

film ^a	h_{max} ^b [nm]	F_{PS} ^c [%]	V_{PS} ^d [nm ³ /μm ²]
a	13 ± 1	35 ± 3	(3.2 ± 0.5) × 10 ⁶
b	7 ± 1	20 ± 3	(1.1 ± 0.5) × 10 ⁶

^a Film a (Figure 3a,b); film b (Figure 3c,d). ^b h_{max} = maxima height of the PS islands. ^c F_{PS} = surface coverage of the PS islands. ^d V_{PS} = PS islands volume per μm².

(Figure 3c,d). The quantitative results of the film analysis are shown in Table 2. The surface coverage of the PS islands and the volume of these islands were determined with the help of a combination of two Nanoscope programs Analyze/Grain Size and Analyze/Bearing from phase contrast and topographic images, respectively. As a ground level of the islands (threshold height) for the volume measurement an average surface level of the surrounding matrix was chosen. The result obtained shows that about 65 ± 5% of PS blocks were removed from the film by selective solvent crazing.

In the case of chain scission at the block junction, the PMMA blocks lose their neighboring PS blocks completely, and PMMA homopolymer remains. Alternatively, PMMA blocks with short PS blocks can be formed if the scission occurs inside the PS phase. This asymmetry should lead to a change of the PMMA behavior during annealing. For films immersed in cyclohexane the PMMA did not form a continuous layer after annealing for 21 h at 150 °C but dewets pointwise the substrate at places, which were covered initially with PS microdomains in the as spin-cast state. The wetting–dewetting situation of the PMMA is a subject of further investigations and will be not discussed in this work.

Phase Identification of the Rim. The diblock film treated by the solvent shows the rims surrounding the initial PS islands in the as spin-cast film. The composition of this elevated rim was investigated as described in the following. A P(S-*b*-MMA) diblock copolymer film was spin-cast identically to the films shown in Figure 1a and Figure 2a,b and was immersed in cyclohexane

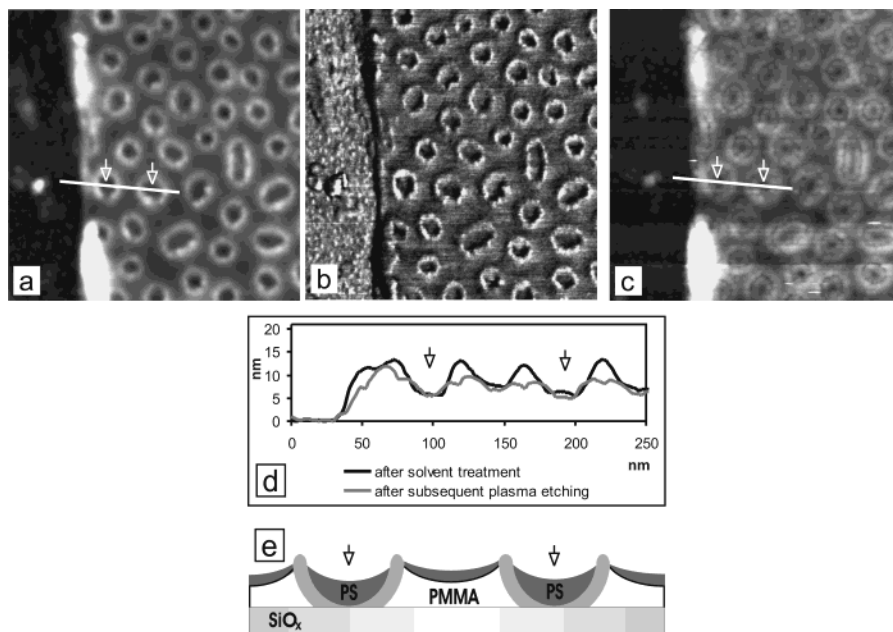


Figure 4. Topographies (a, c) and phase contrast image (b) of an ultrathin P(S-*b*-MMA) diblock copolymer film on silicon substrate, spin-cast (4500 rpm) from MEK solution (2.5 g/L) (a, b) after an immersion in cyclohexane solvent for 1 h at 25 °C (dried 2 h at 50 °C in a vacuum), (c) after subsequent selective etching in air plasma for 15 s; (d) the cross sections of topographic images taken at the positions indicated by white lines in (a) and (c); (e) schematic side view of the film shown in (a). AFM image size: 615 nm × 615 nm. Data scale: height (a, c) 15 nm; phase shift (b) 10°.

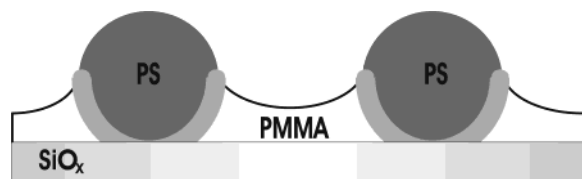


Figure 5. Schematic side view of an ultrathin P(S-*b*-MMA) diblock copolymer film on silicon substrate, spin-cast from MEK solution.

at 25 °C for 1 h. After removal from the solvent the sample was dried in a vacuum and measured by AFM (Figure 4a,b). As can be seen from phase shift image (Figure 4b), the elevated rims have a different (brighter) phase contrast compared to the hollows and the continuous matrix. The same fact can be observed in Figure 2d,f. Three compositional situations can be discussed in principle: first, the rim consists of pure PMMA; second, the rim consists of pure PS that by some reasons has a different phase contrast compared to the other PS; third, the rim consists of both PMMA and PS. To examine the compositional situation in detail, the sample was etched for 15 s in air plasma (Figure 4c). From the comparison of the topographic images (Figure 4a,c) it can be seen that the elevated rims were strongly affected by plasma treatment. The cross sections (Figure 4d) of the film before and after plasma etching reveal that the rims were almost removed. The hollows and the continuous matrix remain almost unaffected because the hollows are filled with PS blocks and the matrix is covered by PS material after the short cyclohexane treatment. Since PMMA is known to be etched by the air plasma faster than PS, it can be concluded on the basis of the obtained results that the rims consist of PMMA or contain a large amount of PMMA. Pure PMMA is not soluble in cyclohexane and stable against the solvent treatment at 25 °C, but cyclohexane seems to influence the rims as can be seen from the comparison of the cross sections of the film after vapor and solvent treatment (Figure 2g). Hence, it can be concluded that the rim is a part of the PS/PMMA interphase. Figure 4e shows a schematic side view of the film morphology after short solvent treatment (Figure 4a) or after cyclohexane vapor treatment (Figure 2c,d) as discussed above.

The selective solvent crazing technique allows to determine the form of the PS/PMMA interface profile, which is covered by the PS domain and dipped into the continuous PMMA matrix in the as spin-cast film. Figure 5 shows a schematic side view of the as spin-cast film in the sense of a logic consequence on the basis of all results obtained from this work, which illustrates the vertical composition in the ultrathin P(S-*b*-MMA) diblock copolymer film on silicon substrate spin-cast from MEK solution.

Conclusion

The morphology of an ultrathin film can be verified by choosing the appropriate solubility parameter of a solvent for the spin-casting procedure. If the solvent is preferentially good for one of the block components, then this component is available for forming the continuous matrix in the spin-cast film; i.e., the resulting continuous phase can be predetermined by choice of the solubility parameter. MEK was chosen as a solvent for the spin-casting procedure to obtain the PS microdomains in a continuous PMMA matrix from the P(S-*b*-MMA) diblock copolymer.

By inspection of solubility parameters of the block components of a diblock copolymer, a solvent for the selective solvent crazing is selected, which shows a dissolution of the cleaved chains of one block component. For selective dissolution of the PS microphase in P(S-*b*-MMA) films the solubility parameters of cyclohexane are appropriate. Some additional investigations show that the observed selective crazing effect is sensitive to time and temperature of the cyclohexane treatment. The contrasting parameters used in this paper are optimized to gain a qualitative viewpoint and to evaluate in-depth information about domain structure. This optimization is done aiming at crazing and selective dissolution of PS microdomains. Alternatively, by etching in air plasma, it is possible to remove selectively the continuous PMMA matrix. Both the contrasting procedures confirm and supplement each other.

Acknowledgment. The helpful discussions with Dr. E. Buck and Priv.-Doz. Dr. J. Adams are greatly appreciated. We are indebted to Prof. Dr. R. Stadler for providing the polymer samples. Financial support by the German National Science Found (DFG) is gratefully acknowledged.

References and Notes

- (1) Van Krevelen, D. W. *Properties of Polymers*, 3rd ed.; Elsevier: Amsterdam, 1990.
- (2) Kambour, R. P.; Gruner, C. L.; Romagosa, E. E. *J. Polym. Sci.* **1973**, *11*, 1897.
- (3) Vincent, P. I.; Raha, S. *Polymer* **1972**, *13*, 283.
- (4) Andrews, E. H.; Bevan, L. *Polymer* **1972**, *13*, 337.
- (5) Bernier, G. A.; Kambour, R. P. *Macromolecules* **1968**, *1*, 393.
- (6) White, S. A.; Weissman, S. R.; Kambour, R. P. *J. Appl. Polym. Sci.* **1982**, *27*, 2675.
- (7) Mayes, A. M.; Johnson, R. D.; Russell, T. P.; Smith, S. D.; Satija, S. K.; Majkrzak, C. F. *Macromolecules* **1993**, *26*, 1047.
- (8) Löwenhaupt, B.; Hellmann, G. P. *Polymer* **1991**, *32*, 1065.
- (9) Nick, L.; Kindermann, A.; Fuhrmann, J. *Colloid Polym. Sci.* **1994**, *272*, 367.
- (10) Nick, L.; Lippitz, A.; Unger, W.; Kindermann, A.; Fuhrmann, J. *Langmuir* **1995**, *11*, 1912.
- (11) Buck, E.; Fuhrmann, J. *Macromolecules* **2001**, *34*, 2172.
- (12) Funaki, Y.; Kumano, K.; Nakao, T.; Jinnai, H.; Yoshida, H.; Kimishima, K.; Tsutsumi, T.; Hirokawa, Y.; Hashimoto, T. *Polymer* **1999**, *40*, 7147.
- (13) Hansen, C. M. *Three-Dimensional Solubility Parameter and Solvent Coefficient. Their Importance in Surface Coating Formulation*; Doctoral Dissertation; Danish Technical Press: Copenhagen, 1967.
- (14) Brandrup, J.; Immergut, E. H. *Polymer Handbook*, 3rd ed.; Wiley Publications: New York, 1991.
- (15) Barton, A. F. M. *Handbook of Solubility Parameters and Other Cohesion Parameters*, 2nd ed.; CRC Press: Boca Raton, FL, 1991.
- (16) Cohen, R. E.; Bates, F. S. *J. Polym. Sci., Polym. Phys. Ed.* **1980**, *18*, 2143.
- (17) Huang, H. Y.; Zhang, F. J.; Hu, Z. J.; Du, B. Y.; He, T. B.; Lee, F. K.; Wang, Y. J.; Tsui, O. K. C. *Macromolecules* **2003**, *36*, 4084.
- (18) Han, C. C.; Mozer, B. *Macromolecules* **1977**, *10*, 44.
- (19) Walheim, S.; Böltau, M.; Mlynek, J.; Krausch, G.; Steiner, U. *Macromolecules* **1997**, *30*, 4995.
- (20) Lin, H.; Steyerl, A.; Satija, S. K.; Karim, A.; Russell, T. P. *Macromolecules* **1995**, *28*, 1470.
- (21) Auschra, C.; Stadler, R.; Voigt-Martin, I. G. *Polymer* **1993**, *34*, 2094.
- (22) Magonov, S. N.; Elings, V.; Whangbo, M.-H. *Surf. Sci. Lett.* **1997**, *375*, L385.
- (23) Binder, K. *Adv. Polym. Sci.* **1999**, *138*, 1.
- (24) Goulon, G.; Daillant, J.; Collin, B.; Benattar, J.; Gallot, Y. *Macromolecules* **1993**, *26*, 1582.